ChemComm

A Molecular Metal Organic Cage as a Recyclable Sponge for PFOS Removal from Water

Journal:	*ChemComm*
Manuscript ID	CC-COM-08-2024-003945.R2
Article Type:	Communication

ChemComm

COMMUNICATION

A Molecular Metal Organic Cage as a Recyclable Sponge for PFOS Removal from Water

Received 00th January 20xx,
Accepted 00th January 20xx

DOI: 10.1039/x0xx00000x

Monojit Das Bairagya,[a] P. Sophie Ntipouna,[a] Natalie K. Stewart,[a] Noémie Elgrishi*[a]

A metal-organic-cage (MOC) is shown to be an efficient molecular sponge for PFOS. A large association constant is observed for the 2:1 PFOS:MOC host-guest complex. Up to 12 equivalents of PFOS per MOC are removed from water. The recycling procedure developed allows for the recovery and reuse of the MOC.

Per- and poly-fluorinated alkyl substances, called PFAS or "forever chemicals" have been used extensively in non-stick cookware, fast food packaging, firefighting foams, paints, shampoo, stain-resistant products, and many other non-slip coatings and anti-foaming agents since the 1950s.[1,2] These compounds are characterized by long fluorinated carbon chains with a carboxylate or sulfonate head and are extremely soluble in water. Common long-chain examples include perfluorooctane sulfonate (PFOS, **Fig. 1**) and perfluorooctanoic acid (PFOA). While the industrial use of PFOS and PFOA has been phased out voluntarily in the USA since the 2000s,[3,4] these compounds continue to accumulate in the environment.[5,6] The stability of the C-F bonds makes PFAS very resistant to degradation, including in the environment.[5,7] Reports mount on the deleterious consequences of PFAS bioaccumulation in humans and other living organisms.[8–14] Many methods have been proposed to degrade PFAS, such as UV irradiation,[15] thermal degradation,[16] and electrochemical oxidation or reduction,[17,18] with varying degrees of success. A recent breakthrough has shown that PFAS can be degraded chemically under certain conditions.[7] However, methods are required first to remove PFAS from drinking water. Many approaches have been developed for this purpose, including separation techniques such as adsorption[19,20] and membrane separation.[21] While some methods are costly and lack selectivity, others lack the ability to regenerate or recycle the materials. Indeed, the higher the affinity for PFAS, —a desired property for PFAS removal— the higher the barrier to recycle the material.

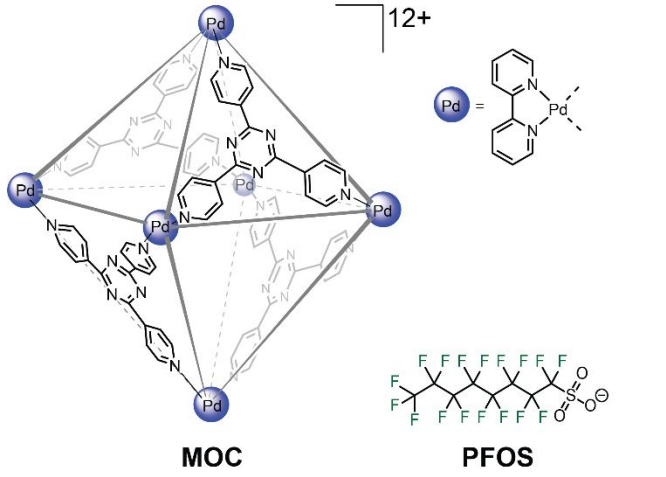

Fig. 1. Structure of the MOC and of PFOS.

Here, we report the interaction between PFOS and a porous metal-organic cage (MOC) in water. Supramolecular chemistry approaches have been used to sequester PFAS in water using cyclodextrin derivatives,[22,23] a water-soluble iron-based,[24] or insoluble Zr-based,[25] molecular cages. In the case of cyclodextrin, up to 2 cyclodextrins are reported to interact with each PFAS molecule. In the case of Fe-based metal-organic cages, 1 equivalent of perfluorohexanoic acid or perfluoroheptanoic acid interacted with the cage in water (1:1 ratios of cage and PFAS). In both cases, recovery of the empty host is challenging.

Here we describe the use of a molecular cage in water to remove 12 equivalents of PFAS per molecular cage, or sponge, and the subsequent removal of the loaded sponge from water and recycling for future use. The specific structure used, **Fig. 1**,

[a] *Department of Chemistry, Louisiana State University, Baton Rouge, Louisiana 70803, United State.*
* Correspondence to: noemie@lsu.edu
Supplementary Information available: [full NMR titrations, DOSY data, Ion-exchange chromatography data, synthesis, and sample preparation details]. See DOI: 10.1039/x0xx00000x

was originally reported and popularized by the pioneering work of Fujita and co-workers.[26]

The structure is composed of 6 metal ions, here palladium, linked by 4 organic ligands on alternating faces of an octahedron. The resulting geometry imparted by the alternating organic panels affords large openings for the encapsulation of guests, and the inside offers a cavity reported to be around 482 Å^3.[27] The cavity is hydrophobic and has been shown to promote aggregation of small water-insoluble neutral fluorinated compounds in water through promoting fluorous interactions in 2014.[28] Given the high and urgent interest in developing new methods to detect, capture, or degrade PFAS, this work investigates the interactions in water between this MOC and PFOS as a test representative of long-chain PFAS.

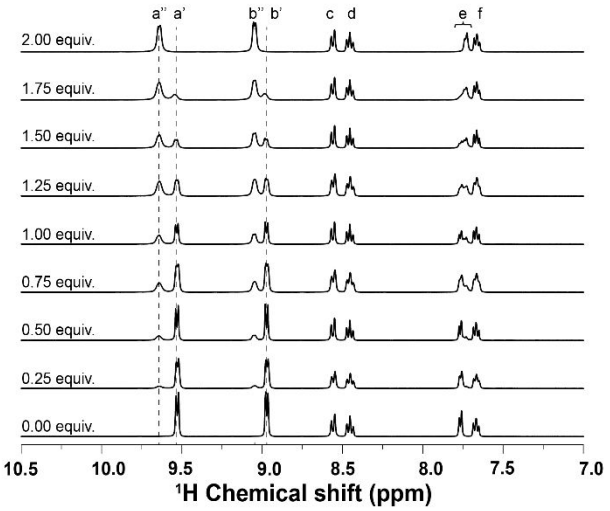

Fig. 2. Evolution of the aromatic region of ^{1}H NMR (400 MHz) data in D_2O of 2.0 mM of the MOC (bottom) in the presence of varying equivalents of PFOS. Full data in Figure S1.

The MOC was dissolved in D_2O, and the ^{1}H NMR resonances of the structure were tracked as PFOS was incrementally added. The evolution of the NMR features (**Fig. 2**) shows the disappearance of the initial resonances as a new population of resonances grows with the addition of PFOS. While changes are observed in most of the NMR resonances of the MOC, the changes are more pronounced in the two groups of resonances labeled a and b, for which a' and b' are fully replaced with a'' and b'' after 2 equivalents of PFOS have been added (**Fig.2**). These resonances are associated with the organic ligand along the faces of the MOC. Meanwhile, resonances c-f corresponding to the bpy ligands around the nodes of the MOC show much smaller changes. These changes are consistent with interactions between the pores of the MOC and PFOS chains. Further additions of PFOS eventually lead to the formation of a white cloudy suspension, which yields the precipitation of a white solid upon further PFOS additions. The solid does not dissolve upon the addition of more water and can easily be recovered by filtration (*vide infra*).

The titration data was further analyzed to obtain a job plot (Figure S2).[29] From the job plot, a stoichiometry of 2 guests for every host is calculated, *i.e.* 2 PFOS per MOC. Overall, these data suggest that the following equilibrium is observed, established rapidly on the time scale of the experiment and with components in slow exchange compared to the NMR time scale: $MOC + 2\ \mathrm{PFOS} \rightleftarrows complex$. In this equation, the complex is 2 PFOS interacting with the MOC. Given the stoichiometry determined and the slow exchange observed, a binding constant can be estimated (SI-7).[29] The equilibrium is very displaced in favor of the complex, and as such the concentration of free PFOS in solution is low in these experiments. This can limit the accuracy of the association constant determination. The binding constant was estimated using the NMR data for the group of resonances a' and a'', as well as for b' and b'', in ranges of PFOS equivalents between 0 and 2. This yielded an average binding constant of $K = 1.93\ (\pm 0.54) \times 10^7\ M^{-2}$ for the resonances a'/a'', while an average value of $K = 1.95\ (\pm 0.62) \times 10^7\ M^{-2}$ was obtained for b'/b'' (Table S1). Of note, the experimental conditions mean that the values obtained represent crude estimations of the lower limit for *K*.

The binding strength between PFOS and the cage was further evaluated through a competition experiment with the organic host β-cyclodextrin (β-CD), which has been reported to bind PFOS in a 2 β-CD to 1 PFOS ratio with a binding affinity of $5.95\times10^4\ M^{-1}$.[30] The competition experiment with 1 equiv. PFOS, 2 equiv. β-CD and 0.5 equiv. MOC confirms the stronger affinity of the MOC compared to β-CD towards binding PFOS (Figure S3). These experiments confirm the very high affinity of the MOC for PFOS in water.

Diffusion-ordered spectroscopy (DOSY) experiments were performed to measure the diffusion coefficient of the free MOC, free PFOS, and MOC:PFOS mixture in a 1:2 ratio (Figure S4-7, Table S2-5). ^{1}H DOSY NMR data were collected to track any changes in the MOC, while ^{19}F DOSY NMR data were used to monitor PFOS in the presence and absence of the MOC. The diffusion coefficients determined from ^{1}H DOSY NMR data were very similar, at 1.45×10^{-10} m^2/s for the free MOC and 1.52×10^{-10} m^2/s for the MOC in the presence of PFOS. This suggests that the hydrodynamic radius of the MOC is not majorly affected by the presence of PFOS. However, the diffusion coefficients determined from ^{19}F DOSY NMR data for PFOS were significantly different in the presence and absence of the MOC. The value of 5.39×10^{-10} m^2/s obtained for free PFOS dropped to 1.31×10^{-10} m^2/s for PFOS in the presence of the MOC, which is close to the values determined for the MOC from ^{1}H DOSY NMR data. These data further confirm a strong interaction between PFOS and the MOC in water.

As discussed above, at low equivalents of PFOS relative to the MOC, we observed host-guest interactions in solution. However, adding further equivalents leads to the appearance of a precipitate. This insoluble material is easily removed from the solution, and the remaining clear filtrate was analyzed through ion exchange chromatography (**Table 1**). A comparison of PFOS concentrations in water before and after treatment with the MOC confirms that PFOS was removed from water. The extent of PFOS removal correlates to the amount of MOC used, with up to 12 PFOS removed per equivalent of MOC.

Table 1. Effect of MOC addition on PFOS concentration.

Entry	MOC (μM)	Initial PFOS (μM)[a]	Final PFOS (μM)	Δ[b] PFOS per MOC
1	4.17	100.7 (± 0.6)	51.3 (± 0.6)	11.8 eq.
2	8.33	99.3 (± 1.5)	n. d.	11.9 eq.
3	16.7	100.7 (± 0.6)	n. d.	6.0 eq.
4	0.104	2.52 (± 0.11)[a]	1.33 (± 0.11)	11.4 eq.
5	0.208	2.52 (± 0.11)[a]	n. d.[c]	12.1 eq.
6	0.417	2.52 (± 0.11)[a]	n. d.[c]	6.0 eq.

All concentrations are the average of 3 measurements. [a]: Measured from the same solution, split across the different experiments in entries 4-6. [b]: change in equivalents of PFOS per equivalent of added MOC. [c]: none detected.

The decrease in PFOS concentration is accompanied by a corresponding increase in the concentration of NO_3^- (Table S6). The NO_3^- originates from the MOC, as each equivalent of the MOC has twelve NO_3^- counter anions. Overall, when PFOS-contaminated water is treated with the MOC, PFOS is replaced with nitrate in up to 12 equivalents per MOC. This is observed both in a high concentration range of ca. 100 μM (**Table 1** entries 1-3) and lower concentration range of ca. 2.5 μM (**Table 1** entries 4-6). In both ranges, as expected, adding fewer than 1/12 equivalents of MOC per PFOS leads to excess PFOS remaining in solution (**Table 1**, entries 1 and 4). Together, these data show that the MOC is effective in removing 12 equivalents of PFOS at varying concentrations.

The white precipitate that forms when the MOC is in the presence of excess PFOS was investigated further. The solid was collected and dried under vacuum. The solid is insoluble in water but dissolves in several organic solvents, including dimethylsulfoxide, acetonitrile, and dimethylformamide. ^{1}H NMR of the solid dissolved in CD_3CN showed resonances consistent with the presence of the MOC (**Fig. 3**). The lack of solubility in acetonitrile of the initial MOC with NO_3^- counter ions precluded the direct comparison with an authentic sample. Meanwhile, ^{19}F NMR of the same sample showed resonances consistent with the presence of free PFOS, suggesting the complex released the PFOS anions in the acetonitrile solvent (Figure S11). Taken together with the observation of the increase in NO_3^- concentration in water upon treatment with the MOC (Table S6), these data confirm that at high concentrations of PFOS, 12 equivalents of PFOS replace the 12 NO_3^- counter anions, with the formation of an insoluble white solid containing 12 equivalents of PFOS per MOC.

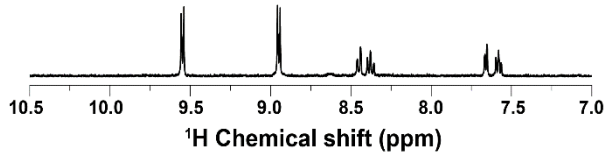

Fig. 3. ^{1}H NMR (400 MHz) spectrum of the obtained MOC and PFOS solid dissolved in CD_3CN.

A recycling procedure was developed to both confirm this hypothesis and recover the starting MOC. The white solid was dissolved in CH_3CN. Tetrabutylammonium nitrate was then added to the clear CH_3CN solution. This caused the formation of a solid, identified by ^{1}H NMR in D_2O as pure MOC. Meanwhile, the filtrate contains the PFOS removed from the initial water treatment, now concentrated in CH_3CN and ready for disposal. The overall process is shown in **Fig. 4**.

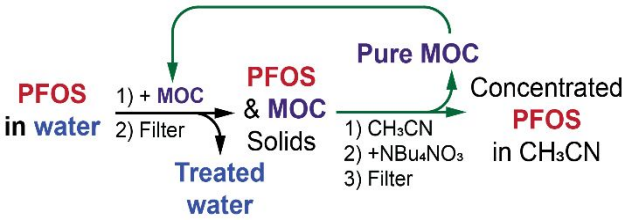

Fig. 4. Schematic representation of the removal of PFOS from water and subsequent recycling of the MOC.

We performed this simple recycling process for three cycles. At the end of the third cycle, the recovered MOC was dried under vacuum. Both ^{1}H and ^{19}F NMRs of the recycled MOC were collected in D_2O (Figure S12-13). The ^{1}H NMR data matched with the authentic MOC sample before the start of the recycling process, while the ^{19}F NMR data didn't show any resonances, supporting the claim that the recovered MOC solid is free from PFOS. Based on the ^{1}H NMR data of the recovered MOC, with ethylene carbonate as an internal standard, 94.5% of the starting MOC was recovered after three cycles. The loss after 3 recycling cycles is expected to be caused by human inaccuracies in sample handling rather than any chemical limitation, confirming the efficacy of the recycling procedure developed.

Finally, the influence of the presence of other anions commonly present in drinking water on the PFOS removal procedure was tested. Specifically, the ability of the MOC to precipitate in the presence of excess PFOS was monitored by UV-vis (**Fig. 5**). The presence of nitrate, fluoride, chloride, phosphate, or sulfate was shown to have a negligible impact on the PFOS removal process.

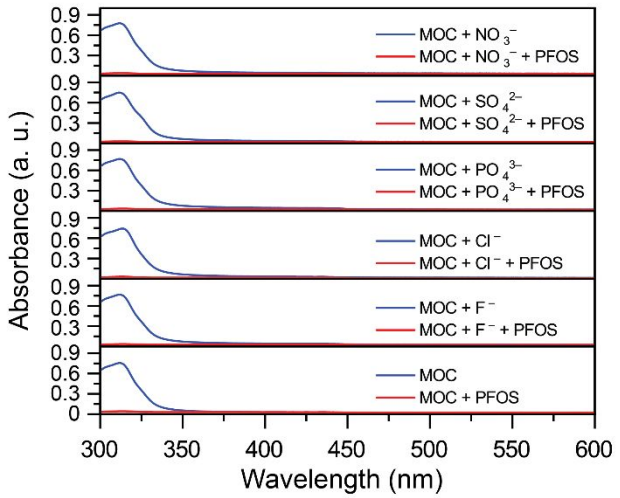

Fig. 5. Impact of the presence of common anions in water on the UV-vis absorption spectrum of 9 μM of the MOC before and after treatment with 18 equivalents of PFOS. The concentration of anions was selected as the limit or typical content in drinking water (Table S7).

Overall, the MOC selected is effective for the removal of PFOS from water, even in the presence of other common anions. It is hypothesized that the large hydrophobic cavity of the MOC can accommodate 2 PFOS based on NMR data. In the presence of higher equivalents of PFOS, 12 PFOS per MOC are precipitated from the solution as a solid. Critically, and in spite of the very large affinity constant for PFOS, the MOC can be recycled and reused. The process yields concentrated PFOS in organic solvents ready for further processing or degradation. More work is required to develop PFOS degradation methods, as well as to move away from precious metals in the nodes of the MOC.[31]

The authors acknowledge support from the College of Science and Department of Chemistry of Louisiana State University (LSU), as well as from the Office of Research & Economic Development through the Workforce and Innovation for a Stronger Economy (WISE)/Act803 fund. The work was also partially supported by a LSU Provost's Fund for Innovation in Research Emerging Research Award. MDB and PSN acknowledge partial support from the National Science Foundation under award number 2046445. PSN acknowledges partial support from the LSU work-study program. We thank Profs. Semin Lee and Víctor García-López for helpful discussions.

Data availability statement

The data supporting this article have been included as part of the Supplementary Information.

Conflicts of interest

There are no conflicts to declare.

Notes and references

1 J. Glüge, M. Scheringer, I. T. Cousins, J. C. DeWitt, G. Goldenman, D. Herzke, R. Lohmann, C. A. Ng, X. Trier and Z. Wang, *Environ. Sci. Process. Impacts*, 2020, **22**, 2345–2373.

2 S. Y. Wee and A. Z. Aris, *npj Clean Water*, 2023, **6**, 57.

3 K. I. Kirkwood-Donelson, J. N. Dodds, A. Schnetzer, N. Hall and E. S. Baker, *Sci. Adv.*, , DOI:10.1126/sciadv.adj7048.

4 J. T. Szilagyi, V. Avula and R. C. Fry, *Curr. Environ. Heal. Reports*, 2020, **7**, 222–230.

5 M. G. Evich, M. J. B. Davis, J. P. McCord, B. Acrey, J. A. Awkerman, D. R. U. Knappe, A. B. Lindstrom, T. F. Speth, C. Tebes-Stevens, M. J. Strynar, Z. Wang, E. J. Weber, W. M. Henderson and J. W. Washington, *Science*, , DOI:10.1126/science.abg9065.

6 I. T. Cousins, J. H. Johansson, M. E. Salter, B. Sha and M. Scheringer, *Environ. Sci. Technol.*, 2022, **56**, 11172–11179.

7 B. Trang, Y. Li, X.-S. Xue, M. Ateia, K. N. Houk and W. R. Dichtel, *Science .*, 2022, **377**, 839–845.

8 M. I. Gomis, R. Vestergren, M. MacLeod, J. F. Mueller and I. T. Cousins, *Environ. Int.*, 2017, **108**, 92–102.

9 E. M. Sunderland, X. C. Hu, C. Dassuncao, A. K. Tokranov, C. C. Wagner and J. G. Allen, *J. Expo. Sci. Environ. Epidemiol.*, 2019, **29**, 131–147.

10 V. Barry, A. Winquist and K. Steenland, *Environ. Health Perspect.*, 2013, **121**, 1313–1318.

11 M. Karlsen, P. Grandjean, P. Weihe, U. Steuerwald, Y. Oulhote and D. Valvi, *Reprod. Toxicol.*, 2017, **68**, 145–153.

12 O. Kuzukiran, I. Simsek, A. Filazi and B. Yurdakok-Dikmen, in *Reproductive and Developmental Toxicology*, Elsevier, 2022, pp. 815–831.

13 D. V. Lind, L. Priskorn, T. H. Lassen, F. Nielsen, H. B. Kyhl, D. M. Kristensen, H. T. Christesen, J. S. Jørgensen, P. Grandjean and T. K. Jensen, *Reprod. Toxicol.*, 2017, **68**, 200–206.

14 N. Jacquet, M. A. Maire, Y. Landkocz and P. Vasseur, *Arch. Toxicol.*, 2012, **86**, 305–314.

15 L. Qian, F.-D. Kopinke and A. Georgi, *Environ. Sci. Technol.*, 2021, **55**, 614–622.

16 L. J. Winchell, J. J. Ross, M. J. M. Wells, X. Fonoll, J. W. Norton and K. Y. Bell, *Water Environ. Res.*, 2021, **93**, 826–843.

17 T. X. H. Le, H. Haflich, A. D. Shah and B. P. Chaplin, *Environ. Sci. Technol. Lett.*, 2019, **6**, 504–510.

18 J. J. Calvillo Solís, C. Sandoval-Pauker, D. Bai, S. Yin, T. P. Senftle and D. Villagrán, *J. Am. Chem. Soc.*, 2024, **146**, 10687–10698.

19 N. Belkouteb, V. Franke, P. McCleaf, S. Köhler and L. Ahrens, *Water Res.*, 2020, **182**, 115913.

20 H. Campos-Pereira, J. Makselon, D. B. Kleja, I. Prater, I. Kögel-Knabner, L. Ahrens and J. P. Gustafsson, *Chemosphere*, 2022, **297**, 134167.

21 A. Zaggia, L. Conte, L. Falletti, M. Fant and A. Chiorboli, *Water Res.*, 2016, **91**, 137–146.

22 M. J. Weiss-Errico, I. Ghiviriga and K. E. O'Shea, *J. Phys. Chem. B*, 2017, **121**, 8359–8366.

23 Z. Chen, Y.-L. Lu, L. Wang, J. Xu, J. Zhang, X. Xu, P. Cheng, S. Yang and W. Shi, *J. Am. Chem. Soc.*, 2023, **145**, 260–267.

24 C. R. P. Fulong, M. G. E. Guardian, D. S. Aga and T. R. Cook, *Inorg. Chem.*, 2020, **59**, 6697–6708.

25 D. Camdzic, H. K. Welgama, M. R. Crawley, A. Avasthi, T. R. Cook and D. S. Aga, *ACS Appl. Eng. Mater.*, 2024, **2**, 87–95.

26 W.-Y. Sun, T. Kusukawa and M. Fujita, *J. Am. Chem. Soc.*, 2002, **124**, 11570–11571.

27 Y. Fang, T. Murase, S. Sato and M. Fujita, *J. Am. Chem. Soc.*, 2013, **135**, 613–615.

28 H. Takezawa, T. Murase, G. Resnati, P. Metrangolo and M. Fujita, *J. Am. Chem. Soc.*, 2014, **136**, 1786–1788.

29 K. Hirose, in *Analytical Methods in Supramolecular Chemistry*, Wiley, 2012, vol. 1, pp. 27–66.

30 M. J. Weiss-Errico and K. E. O'Shea, *J. Hazard. Mater.*, 2017, **329**, 57–65.

31 C. E. Hauke, A. N. Oldacre, C. R. P. Fulong, A. E. Friedman and T. R. Cook, *Inorg. Chem.*, 2018, **57**, 3587–3595.

Data availability

The data supporting this article have been included as part of the Supplementary Information.